© 2017. Published by The Company of Biologists Ltd | Development (2017) 144, 3907-3916 doi:10.1242/dev.150086

STEM CELLS AND REGENERATION

RESEARCH ARTICLE

Macrophages are required to coordinate mouse digit tip regeneration

Jennifer Simkin[1,*,§], Mimi C. Sammarco[1,‡,§], Luis Marrero[2], Lindsay A. Dawson[1,3], Mingquan Yan[1,3], Catherine Tucker[1], Alex Cammack[1] and Ken Muneoka[1,3,¶]

ABSTRACT

In mammals, macrophages are known to play a major role in tissue regeneration. They contribute to inflammation, histolysis, re-epithelialization, revascularization and cell proliferation. Macrophages have been shown to be essential for regeneration in salamanders and fish, but their role has not been elucidated in mammalian epimorphic regeneration. Here, using the regenerating mouse digit tip as a mammalian model, we demonstrate that macrophages are essential for the regeneration process. Using cell-depletion strategies, we show that regeneration is completely inhibited; bone histolysis does not occur, wound re-epithelialization is inhibited and the blastema does not form. Although rescue of epidermal wound closure in the absence of macrophages promotes blastema accumulation, it does not rescue cell differentiation, indicating that macrophages play a key role in the redifferentiation of the blastema. We provide additional evidence that although bone degradation is a component, it is not essential to the overall regenerative process. These findings show that macrophages play an essential role in coordinating the epimorphic regenerative response in mammals.

KEY WORDS: Regeneration, Mammal, Epimorphic, Blastema, Macrophage, Osteoclasts

INTRODUCTION

All animals display some level of regenerative ability, but this capacity varies substantially. Among vertebrates, urodele amphibians possess the ability to faithfully regenerate large parts of their body, for example their limbs (Brockes, 1997), while a number of fish species, including zebrafish, readily regenerate their tail fins (Gemberling et al., 2013; Pfefferli and Jaźwińska, 2015). These examples involve the coordinated regeneration of multiple tissues. This process is mediated by the formation of a blastema, a heterogeneous population of cells that can re-enter the cell cycle and reutilize developmental mechanisms to replace lost structures (Brockes and Kumar, 2002; Bryant et al., 2002; Stocum and Cameron, 2011; Tanaka, 2003). Blastema-mediated regeneration, termed epimorphic, is considered to be distinct from the regeneration of individual damaged tissues, such as skin and bone, which undergo a repair response without forming a blastema (Carlson, 2005). In general, mammals display tissue-specific regenerative abilities (e.g. healing bone fractures) but a limited capacity to coordinate a multi-tissue regenerative response.

Among mammals there are only a few models of epimorphic regeneration, and the developing and adult digit tip of the mouse is the best characterized (Borgens, 1982; Fernando et al., 2011; Han et al., 2008; Neufeld and Zhao, 1993). Digit tip regeneration in mice parallels the regeneration of human fingertips, a process well documented in the clinical literature (Illingworth, 1974; McKim, 1932), and displays characteristics that are similar to amphibian models of limb regeneration, including blastema formation (Fernando et al., 2011; Han et al., 2008). Amputation of an adult mouse terminal phalangeal element (P3) transects the nail plate, epidermis, dermis (which includes loose connective tissue), blood vessels and nerves, bone, and bone marrow (Simkin et al., 2013). Thus, the primary structural tissues that regenerate are bone, including bone marrow, and skin, including epidermis and its derivatives as well as the heterogeneous dermis. When studied as separate tissues, skin and bone undergo very different healing responses than that observed during the coordinated multi-tissue digit regeneration response.

The repair of mammalian skin has been studied primarily in full-thickness wounds in which the healing response consists of distinct but overlapping phases beginning with hemostasis/inflammation, the formation of granulation tissue and, finally, matrix remodeling (Eming et al., 2014). The inflammatory response dominates the early stages of healing and is crucial for re-epithelialization as well as supporting the formation of granulation tissue (DiPietro et al., 1998; Goren et al., 2009; Leibovich and Ross, 1975; Mirza et al., 2009). Later, during matrix remodeling, the immature scar tissue deposited by granulation tissue is realigned and cross-linked to form the mature scar (Xue and Jackson, 2015). The wound healing process involves a balance between inflammatory and anti-inflammatory signals but overall is not considered regenerative (i.e. dermal patterning is not restored and epidermal structures do not regrow), and depletion of macrophages, neutrophils and inflammatory signals results in less granulation tissue formation and a scar-free regenerative healing response (Ashcroft et al., 1999; Martin et al., 2003; Mori et al., 2002). Thus, high numbers of macrophages appear to function in an inhibitory way. Alternatively, tissue-specific bone regeneration has been studied in the context of fracture healing and consists of distinct overlapping phases, which begins with inflammation and ends with remodeling of the regenerated bone (Schindeler et al., 2008). Macrophage depletion studies show that these cells are required for bone regeneration and successful fracture healing (Alexander et al., 2011; Raggatt et al., 2014). Thus, in a bone regeneration model, macrophages play an essential and stimulatory role in the regeneration of new bone.

It is not intuitively obvious how the epimorphic regenerative properties of the digit tip relate to the tissue-specific repair properties

[1]Division of Developmental Biology, Department of Cell and Molecular Biology, Tulane University, New Orleans, LA 70118, USA. [2]Morphology and Imaging Core Laboratory, Louisiana Health Sciences Center, New Orleans, LA 70112, USA. [3]Department of Veterinary Physiology and Pathology, College of Veterinary Medicine, Texas A&M University, College Station, TX 77843, USA.
*Present address: Department of Biology, University of Kentucky, Lexington, KY 40508, USA. ‡Present address: Department of Surgery, Tulane School of Medicine, New Orleans, LA 70112, USA.

§These authors contributed equally to this work

¶Author for correspondence (kmuneoka@cvm.tamu.edu)

K.M., 0000-0002-7520-6869

Received 20 February 2017; Accepted 8 September 2017

Development (2017) 144, 3907-3916 doi:10.1242/dev.150086

of bone (regenerative) and skin (non-regenerative). Nevertheless, both repair responses initiate with inflammation; in the case of wound healing, its action is largely inhibitory, whereas in fracture healing its action is stimulatory. Inflammation in mammalian epimorphic regeneration has not been investigated, although recent studies in urodele limb and zebrafish fin regeneration show that macrophages are required for regeneration (Godwin et al., 2013; Petrie et al., 2014). We use the mouse digit tip to investigate the effects of macrophages during a mammalian epimorphic regeneration response. In this study, we focus on cells of the monocytic lineage, including macrophages and osteoclasts. Monocytic cell depletion inhibits bone degradation, wound re-epithelialization, blastema formation and completely inhibits the regenerative response. Conversely, enhancing macrophage numbers does not have a major effect on the regeneration response. Coupling monocyte cell depletion with the rescue of wound re-epithelialization rescues blastema formation but does not rescue regeneration. On the other hand, targeted depletion of osteoclasts coupled with rescuing wound re-epithelialization inhibits bone degradation but does not inhibit blastema formation and regeneration. Thus, if wound re-epithelialization is stimulated, regeneration occurs in the absence of active osteoclasts but not in the absence of active macrophages. With these data we conclude that wound re-epithelialization is a macrophage-dependent process that is required for blastema accumulation. Finally, these results suggest that macrophages play a prominent role in the redifferentiation stage of regeneration, independent of a role in osteoclastogenesis or wound re-epithelialization.

RESULTS

Both neutrophils and macrophages accumulate at the injury site after digit amputation

To characterize the inflammation response following mouse digit amputation, immunohistochemical techniques were used to analyze the timing and position of CD45$^+$ (PTPRC$^+$) hematopoietic cells, Ly6B.2$^+$ neutrophils (Hirsch and Gordon, 1983) and F4/80$^+$ (ADGRE1$^+$) macrophages (Austyn and Gordon, 1981) within the amputation wound (Fig. 1A). Wound closure following digit tip amputation is a lengthy process that takes 8-9 days and involves circumferential healing of the epidermis onto dead stump bone (Fernando et al., 2011; Simkin et al., 2015). The cells of the amputation wound response are therefore localized to the periphery of the amputated P3 bone. Prior to and immediately following amputation, there are few neutrophils or macrophages present in the mature digit (Fig. 1B,F). Indeed, there are few CD45$^+$ cells in the mature digit indicating that the pool of resident cells of the hematopoietic cell lineage prior to amputation injury is very low (Fig. 1J). Following amputation we find a progressive influx of neutrophils within digit stump tissues that peaks at 5 days post amputation (DPA) (ANOVA, main effect time, F=10.54, P=0.0002; Bonferroni post-hoc test, P<0.05). Ly6B.2$^+$ cells associated with the scab at 3 DPA appear to be dead or dying, while neutrophils present in the stump are mainly present in the bone marrow cavity (Fig. 1C, arrowheads). At 7 DPA, the wound epidermis is not yet closed; neutrophils are localized to the bone marrow and the dermal connective tissue surrounding the bone stump (Fig. 1D). When the blastema forms by 10 DPA, neutrophils are predominately localized to the blastema and the bone marrow cavity (Fig. 1E). By 15 DPA, neutrophil numbers return to pre-amputation levels (Fig. 1A).

Following digit amputation, macrophage numbers peak at 7 DPA and return to baseline by 21 DPA (Fig. 1A; ANOVA, main effect time, F=3.18, P=0.04; Bonferroni post-hoc test, P<0.05). The spatial localization of F4/80$^+$ cells at selected time points was somewhat variable across animals and this is reflected in Fig. 1. We did however notice a few trends. F4/80$^+$ cells are seen in low numbers in the bone marrow immediately following amputation (Fig. 1F). At 3 DPA, macrophages are scattered within the bone marrow and also in the connective tissue surrounding the P3 stump (Fig. 1G). At 7 and

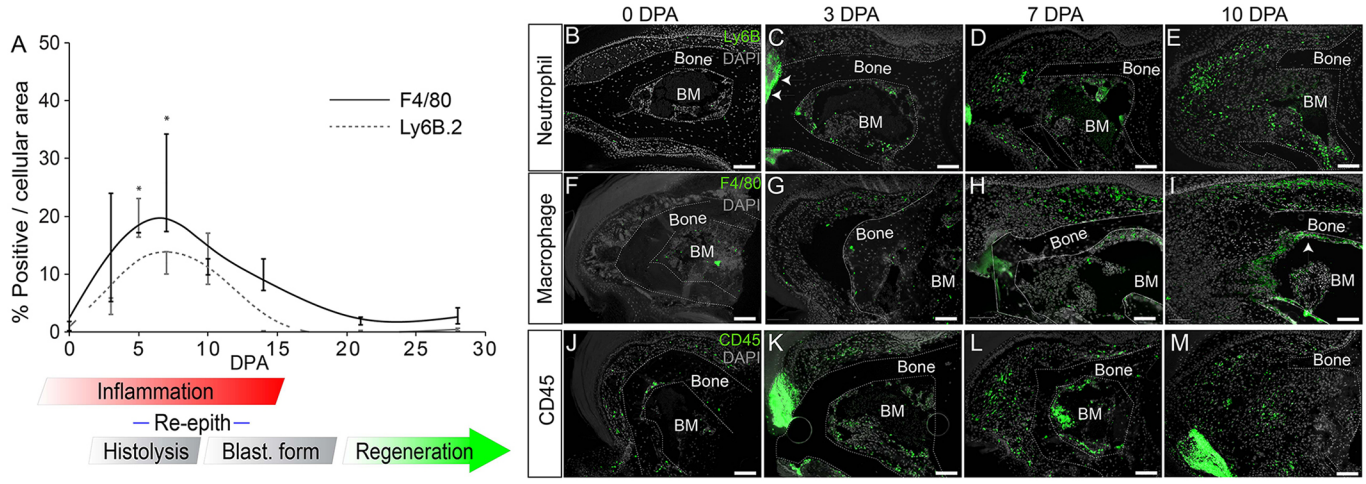

Fig. 1. Leukocytes are recruited to the injury site after amputation. (A) Macrophage and neutrophil numbers are quantified using immunohistochemistry for the pan-macrophage marker F4/80 and the neutrophil cell surface protein Ly6B.2. Both macrophage and neutrophil numbers increase at the wound site temporarily following a regenerative P3 amputation. Stages of regeneration are delineated beneath the graph: inflammation, histolysis, re-epithelialization, blastema formation, regeneration. Bonferroni post-hoc test, *P<0.05 for Ly6B.2 0 DPA versus 5 DPA and for F4/80 0 DPA versus 7 DPA. n=3 per time point. Error bars indicate s.e.m. (B-E) Ly6B.2$^+$ cells (green) are observed in the injury area after amputation, in low numbers at 0 DPA (B), in the bone marrow and in scab (arrowheads) at 3 DPA (C), and in the forming blastema and bone marrow at 7 DPA (D) and 10 DPA (E). (F-I) F4/80$^+$ macrophages (green) are observed in low numbers at 0 DPA (F) and 3 DPA (G). At 7 DPA, F4/80$^+$ macrophages localize to the soft connective tissue surrounding the bone stump and in the bone marrow (H). By 10 DPA the blastema is formed and F4/80$^+$ macrophages are present in the connective tissue surrounding the bone stump and lining the endosteal layer (arrowhead) of the bone marrow cavity (I). F4/80$^+$ macrophages are notably absent from the blastema proper. (J-M) Presence of CD45$^+$ leukocytes (green) surrounding the P3 digit is low at 0 DPA (J) and increases after amputation at 3 (K), 7 (L) and 10 (M) DPA. Gray, DAPI nuclear stain. For all images: distal, left; dorsal, top. DPA, days post amputation; BM, bone marrow. Scale bars: 100 µm.

Development (2017) 144, 3907-3916 doi:10.1242/dev.150086

10 DPA, macrophages are found in high numbers within the dermis associated with the nail matrix, and by 10 DPA F4/80$^+$ cells also line the endosteal layer of the P3 bone marrow (Fig. 1H,I). Notably, once the blastema forms, few F4/80$^+$ macrophages are observed in the blastema itself (Fig. 1I) and this was consistent across all regenerates analyzed. Immunohistochemical staining of the pan-hematopoietic marker CD45 at similar regeneration stages identifies cells within the bone marrow, stump dermis, and blastema that overlap the combined staining for neutrophils and macrophages (Fig. 1K-M), suggesting that these cell types represent the majority of the hematopoietic response to digit amputation. Overall, the regeneration response is associated with an accumulation of neutrophils found predominately within the bone marrow and blastema, while macrophages are localized initially to the stump dermis associated with the nail matrix, and later to the endosteum of the P3 bone stump.

Macrophages are required for digit tip regeneration

To explore the role that the macrophage population has in digit tip regeneration, we first tested the hypothesis that increasing macrophage presence inhibits regenerative capacity. We used targeted application of monocyte chemoattractant protein 1 (MCP1; also known as CCL2) following digit tip amputation to enhance the recruitment of activated macrophages (Dipietro et al., 2001). A microcarrier bead soaked in a high concentration of MCP1 (0.5 µg/µl) was implanted in the connective tissue of the P3 digit. In uninjured digits this MCP1 treatment is able to enhance macrophage recruitment over control BSA-treated beads at 5 days post implantation (DPI), and macrophage levels returned to control levels by 15 days (Fig. 2A; Bonferroni post-hoc test, main effect treatment, $P<0.05$). When MCP1 treatment was coupled with digit amputation, we observed a higher influx of macrophage numbers compared with BSA-treated digits at 5 and 15 DPA (Fig. 2A; Bonferroni post-hoc test, main effect treatment, $P<0.05$). The enhanced macrophage presence was observed in both the dermis and bone marrow (Fig. 2B,C). These data show that MCP1 treatment successfully enhances and sustains macrophage recruitment to the regenerating amputation wound.

Following the regeneration process using µCT *in vivo* imaging, we found that MCP1-treated digits successfully regenerated largely in parallel with controls (Fig. 2D,E). Bone volume measurements during the regenerative response indicated a statistically significant reduction in bone degradation associated with MCP1 treatment (Fig. 2D; Bonferroni post-hoc test, main effect treatment, $P<0.05$). This result was not anticipated based on evidence that MCP1 enhances osteoclast differentiation *in vitro* and also enhances foreign body-giant cell fusion *in vivo* (Khan et al., 2016; Kyriakides et al., 2004). Nevertheless, the findings indicate that enhancing F4/80$^+$ macrophage recruitment to the amputated digit does influence monocyte lineage cells but does not inhibit the regenerative response. These data do not support the hypothesis that macrophages are inhibitory for regeneration in mammals.

To explore the effect of depleting macrophage numbers during digit tip regeneration we used a commercially available reagent, clodronate liposomes, that is effective in transiently depleting macrophages when applied either systemically or locally (Alexander et al., 2011; Barrera et al., 2000; Li et al., 2013; Xiang et al., 2012). Clodronate liposomes are selectively engulfed by phagocytic cells and are cell lethal; however, unengulfed

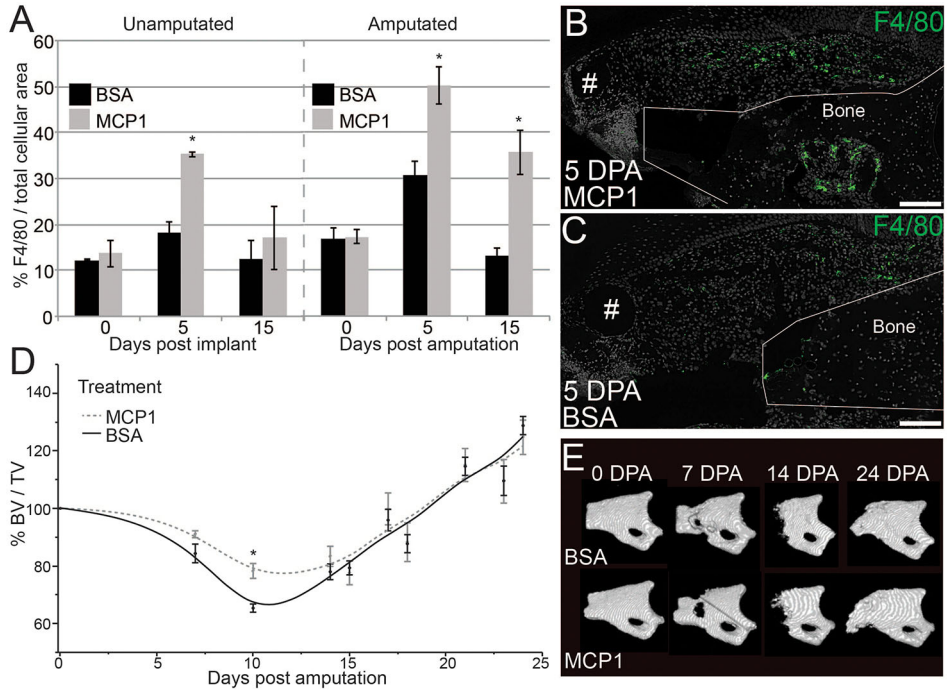

Fig. 2. Increasing macrophage numbers does not inhibit regenerative ability. (A) The introduction of monocyte chemoattractant protein 1 (MCP1) via a microcarrier bead is able to recruit a higher number of F4/80$^+$ cells to P3 compared with BSA control beads both in unamputated digits and following amputation. *y*-axis, total area of F4/80 signal per total area of DAPI signal in the connective tissue area. *x*-axis, days post bead implantation in unamputated and amputated digits. $n=7$ mice, 14 digits per treatment. Bonferroni post-hoc test, $^*P<0.05$ for main effect treatment. Error bars indicate s.e.m. (B,C) Immunofluorescence with anti-F4/80 at 5 DPA after implantation of microcarrier beads soaked in MCP1 (B) or BSA (C). Green, F4/80; gray, DAPI; #, microcarrier bead. Scale bars: 100 µm. (D) µCT analysis of bone volume change over time. MCP1-treated digits show a significant reduction in the amount of bone degradation when compared with BSA controls, but show the same overall bone volume growth by DPA 24 as compared with BSA controls. *y*-axis, percent bone volume per total volume at time of amputation (%BV/TV). $n=7$ mice, 14 digits per treatment. Bonferroni post-hoc test, $^*P<0.05$ for main effect treatment. (E) 3D renderings of µCT data show patterned bone growth in both BSA-treated and MCP1-treated digits by 24 DPA. For all images: distal, left; dorsal, top.

Development (2017) 144, 3907-3916 doi:10.1242/dev.150086

liposomes are rapidly cleared (within 15 min) via the kidneys (van Rooijen and Hendrikx, 2010). We used a local clodronate liposome treatment of individual mouse digits during the rise in macrophage recruitment to test whether phagocytic cells are required for digit tip regeneration. Clodronate liposomes (Clo-Lipo) or control liposomes containing PBS (PBS-Lipo) were injected into amputated digits at 0, 2 and 5 DPA. Samples were collected at 6 DPA to check for neutrophil and macrophage presence based on immunohistochemistry and for osteoclast presence based on distinct cytological characteristics, i.e. multinucleated giant cells with ruffled borders. We observed a significant reduction in F4/80^{+} cells in Clo-Lipo-injected digits as compared with PBS-Lipo controls, indicating that targeted treatment effectively diminished, but did not eliminate, the local macrophage population (Fig. 3A; unpaired Student's *t*-test, $P<0.05$). Osteoclasts, which are derived from the monocyte/macrophage lineage (Sprangers et al., 2016) and are known to be present in high numbers during regeneration (Fernando et al., 2011; Sammarco et al., 2014), were also depleted; a finding consistent with Clo-Lipo use in fracture healing (Alexander et al., 2011; Winkler et al., 2010). Neutrophils and osteoblasts are largely unaffected by Clo-Lipo treatment (Fig. S1). These findings show that Clo-Lipo treatment is effective in locally depleting the injury-induced macrophage population.

To evaluate the effect of macrophage and osteoclast depletion on digit regeneration, we tracked anatomical and volumetric changes of the amputated P3 bone with µCT in Clo-Lipo-treated and PBS-Lipo-treated digits (Fig. 3B). 3D renderings of µCT scans show no change in bone architecture or bone volume over a 35 day period following amputation and Clo-Lipo treatment (Fig. 3B,C). Control digits exhibited a regeneration response similar to that reported in previous studies that included an initial bone volume decline prior to blastema formation followed by an average regrowth of 150% of the amputated stump bone volume (Fernando et al., 2011; Sammarco et al., 2014, 2015; Simkin et al., 2015), thus indicating that the liposome vehicle did not alter the regenerative response (Fig. 3B,C). The data show that Clo-Lipo treatment inhibits both the bone degradation response and the regeneration of distal bone.

We also carried out studies to explore the effects of dose and timing of Clo-Lipo treatment on the regeneration response. A single injection of Clo-Lipo at the time of amputation resulted in digits that either failed to regenerate (37.5%; 3/8) or regenerated abnormally (62.5%; 5/8) producing boney spikes from regions of the stump (Fig. S2A). Bone architecture suggests that the degradation phase is completely inhibited by a single treatment with Clo-Lipo, and that bone redifferentiation by the blastema is not an all-or-none event. To explore the relationship between the Clo-Lipo effect and the timing of the inflammation response, a single treatment with Clo-Lipo was administered at the peak of the inflammation response (7 DPA). Treatment at this time shows a trend toward reduced bone degradation and redifferentiation responses, but treated samples were not statistically different from PBS-Lipo-treated controls (Fig. S3; two-way ANOVA, main effect time, $F=25.72$, $P<0.0001$; and main effect treatment, $F=0.002$, $P=0.97$).

These studies identify the early stages of the inflammation response as being critical for the regeneration-promoting effect that phagocytic and histolytic cells, such as macrophages and osteoclasts, have on blastema formation and digit tip regeneration in mice.

Epidermal closure and histolysis are suspended by Clo-Lipo treatment

To better understand Clo-Lipo-inhibited regeneration we carried out a histological analysis on samples that were treated with Clo-Lipo or PBS-Lipo and focused on key stages of the normal regenerative response (Fig. 4). PBS-Lipo-treated digits demonstrate a regenerative response similar to that of untreated digits characterized in previous publications (Fernando et al., 2011; Sammarco et al., 2014, 2015; Simkin et al., 2015). Briefly, at 7 DPA control digits show an open amputation wound, extensive stump bone degradation associated with osteoclast-filled bone pits, a hypercellular bone marrow and activated osteoblasts lining the endosteum and periosteum (Fig. 4A). At 10 DPA the control digits have a closed wound epidermis, a prominent blastema and histological evidence of new osteoid deposition in the interface between the proximal blastema and the stump (Fig. 4B). At 13 DPA new bone growth in the form of woven bone islands is prominent at the blastema/stump interface (Fig. 4C, arrowheads). At 28 DPA the regeneration of control digits is largely complete, with the replacement of the digit tip that consists of newly regenerated

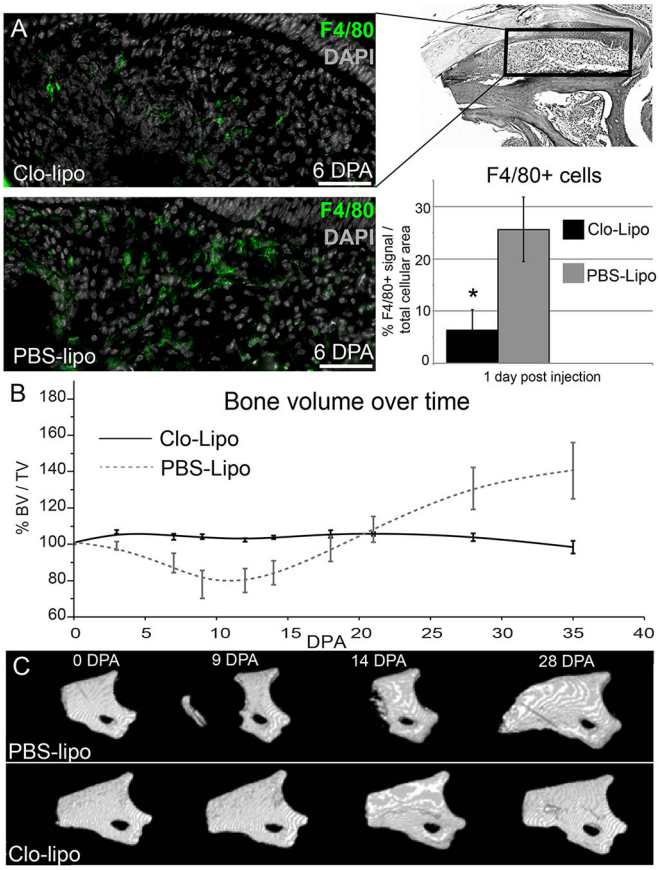

Fig. 3. Local injections of clodronate liposomes effectively deplete macrophage populations and inhibit regeneration. (A) Clodronate liposomes (Clo-Lipo) or PBS liposomes (PBS-Lipo) were locally injected (50 µg) into the P2 digit at 0, 2 and 5 DPA. Quantification of F4/80^{+} cells at 6 DPA (1 day post final injection) reveals a significant reduction in the number of activated macrophages in P3. Green, F4/80; gray, DAPI. Scale bar: 50 µm. *y*-axis, percent F4/80 signal per total DAPI signal in the connective tissue area. Unpaired Student's *t*-test, *$P<0.05$. Error bars indicate s.e.m. (B) µCT analysis of bone volume changes over time shows that PBS-Lipo-treated animals have a normal regeneration response, which includes first a loss of bone volume followed by bone regeneration ($n=4$ mice, 16 digits). By contrast, Clo-Lipo-treated animals exhibit a complete inhibition of both bone degradation and bone regrowth over the course of 35 DPA ($n=4$ mice, 16 digits). (C) 3D renderings of µCT scans enable visualization of the bone loss and regeneration in PBS-Lipo-treated animals. In Clo-Lipo-treated animals, there are no significant changes to bone architecture. For all images: distal, left; dorsal, top.

Development (2017) 144, 3907-3916 doi:10.1242/dev.150086

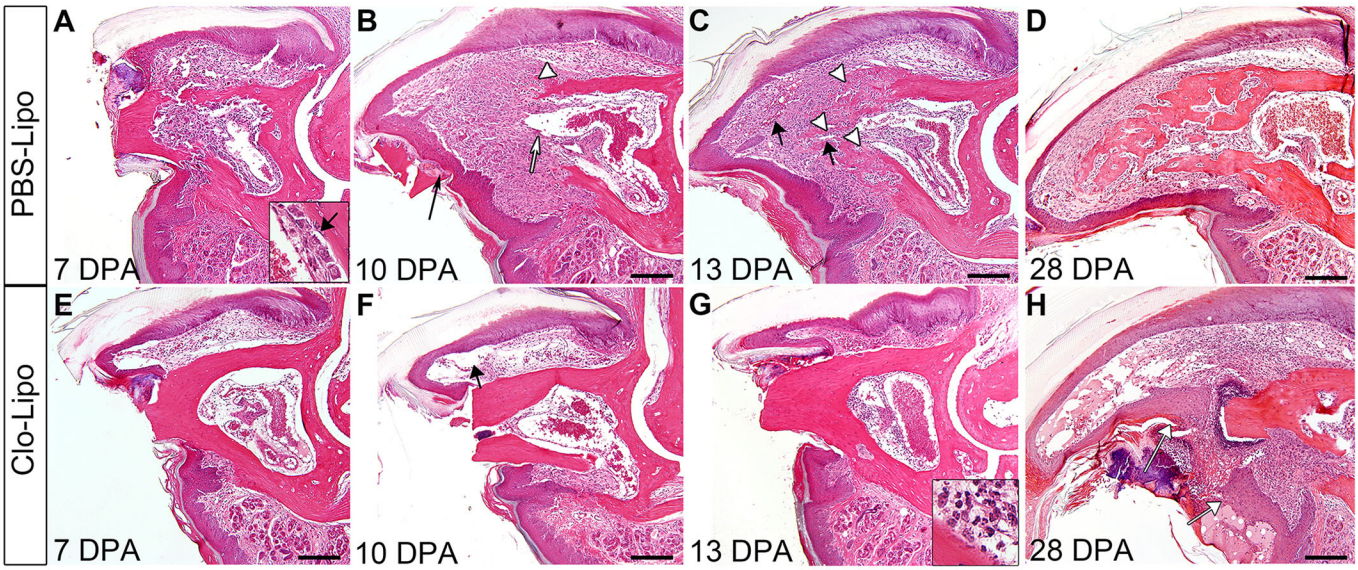

Fig. 4. Injections of clodronate liposomes inhibit histolysis and epidermal closure. (A-D) H&E staining of P3 digits over the course of regeneration in PBS-Lipo-treated digits. By 7 DPA (A), digits display bone degradation and endosteal activation (inset, arrow). By 10 DPA (B), digits have a closed epidermis that ejects degraded bone fragments (black arrow), blastema formation contiguous with the bone marrow (white arrow), and the beginnings of new bone formation (white arrowhead). By 13 DPA (C), new blood vessels have formed (arrows) distal to the newly regenerating bone (arrowheads). By 28 DPA (D), bone continues to be remodeled in trabecular islands. (E-H) H&E staining of P3 digits following Clo-Lipo injections shows an open epidermis and lack of bone degradation at 7 DPA (E). Distal nail and epidermal growth (arrow) is evident at 10 DPA (F) but not epidermal closure. At 13 DPA, there is a lack of re-epithelialization, no bone degradation is observed and no blastema formation is evident. Cell accumulation in the marrow consists of polymorphonuclear cells (inset). The epidermis has failed to close by 28 DPA (H, arrows), although distal epidermal and nail growth is evident. For all images: distal, left; dorsal, top. Scale bars: 200 µm.

woven bone, a re-established distal marrow cavity, regenerated dermis and a regenerated distal nail plate (Fig. 4D).

In sharp contrast, the histology of Clo-Lipo-treated digits shows that the digit stump is largely unchanged during this 28 day period, and that the injury is suspended at an early phase of regeneration (Fig. 4E-H). There are a number of remarkable observations. First, there is no evidence of osteoclasts or bone pitting of the stump at any of the time points analyzed, and this is consistent with bone volume measurements from µCT imaging (Fig. 2B). Thus, Clo-Lipo treatment completely inhibits osteoclastogenesis and bone degradation typically associated with the regenerative response. Second, the epidermis fails to close over the amputation wound even by 28 DPA (Fig. 4H, arrows), indicating that Clo-Lipo treatment inhibits wound closure. However, the nail continues to elongate and creates a large distal pocket devoid of cells subjacent to the elongating nail (Fig. 4F, arrow). Thus, epidermal expansion and nail elongation do not appear to be dependent on either macrophages or the histolytic event. Third, we observe polymorphonuclear neutrophils associated with the amputation wound site (Fig. 4G, inset) at all stages analyzed, suggesting that inflammation characteristics of the amputation wound are maintained and not completely resolved. Fourth, there is no histological evidence of blastema formation and no digit regeneration. Combined, these data suggest that disruption of the regenerative phase by Clo-Lipo-mediated depletion of macrophages and osteoclasts inhibits regeneration.

The specific loss of osteoclasts delays bone degradation and results in impaired regeneration

Osteoclasts are multinucleated cells of the monocyte lineage, so their absence in Clo-Lipo studies was anticipated; however, this combined depletion makes it difficult to differentiate between the effects of depleted macrophages and the effects of depleted osteoclasts. To further elucidate the influence of macrophages on digit regeneration we treated digits with free clodronate (F-Clo), which directly targets osteoclasts for depletion without affecting macrophages (Russell and Rogers, 1999). To establish the efficacy of F-Clo, we administered a single injection into the digit at the time of amputation and evaluated osteoclast and macrophage presence at 7 DPA. Immunohistochemical studies show a distinct reduction of cathepsin K^+ osteoclasts when compared with PBS-injected control digits (Fig. 5A,B). By contrast, $F4/80^+$ macrophages were abundant at the distal stump of P3 in F-Clo-treated and PBS-treated control digits (Fig. 5C,D). These data show that F-Clo treatment is effective in selectively depleting osteoclasts without impairing the macrophage population during digit tip regeneration, and this result is consistent with previous reports (Frith et al., 1997; Zeisberger et al., 2006).

To study the effect of F-Clo on digit regeneration we measured changes in bone volume using µCT imaging following a single treatment with F-Clo at the time of amputation. Control digits injected with PBS undergo a normal regeneration response as previously described (see Fig. 2C,D). By contrast, digits receiving a single injection with F-Clo displayed an impaired regeneration response characterized by a delay in the onset of bone degradation and a reduced osteogenic response (Fig. 5E,F; Bonferroni post-hoc test, main effect treatment, $P<0.05$). Histological analysis at 11 DPA and 14 DPA showed that wound closure, blastema formation and regeneration are delayed in F-Clo-treated digits (Fig. 5G).

To address the hypothesis that regeneration is dependent on osteoclasts and bone degradation, we took advantage of our previous finding that the degradation/re-epithelialization link can be uncoupled by stimulating rapid wound closure over the amputated stump with the cyanoacrylic wound dressing Dermabond (Simkin et al., 2015). To determine if osteoclasts are necessary for blastema formation and regeneration downstream of wound closure, we treated osteoclast-depleted and control digits with Dermabond. Based on histological analyses, applying Dermabond to F-Clo-treated or PBS-treated digits stimulated epidermal closure

Development (2017) 144, 3907-3916 doi:10.1242/dev.150086

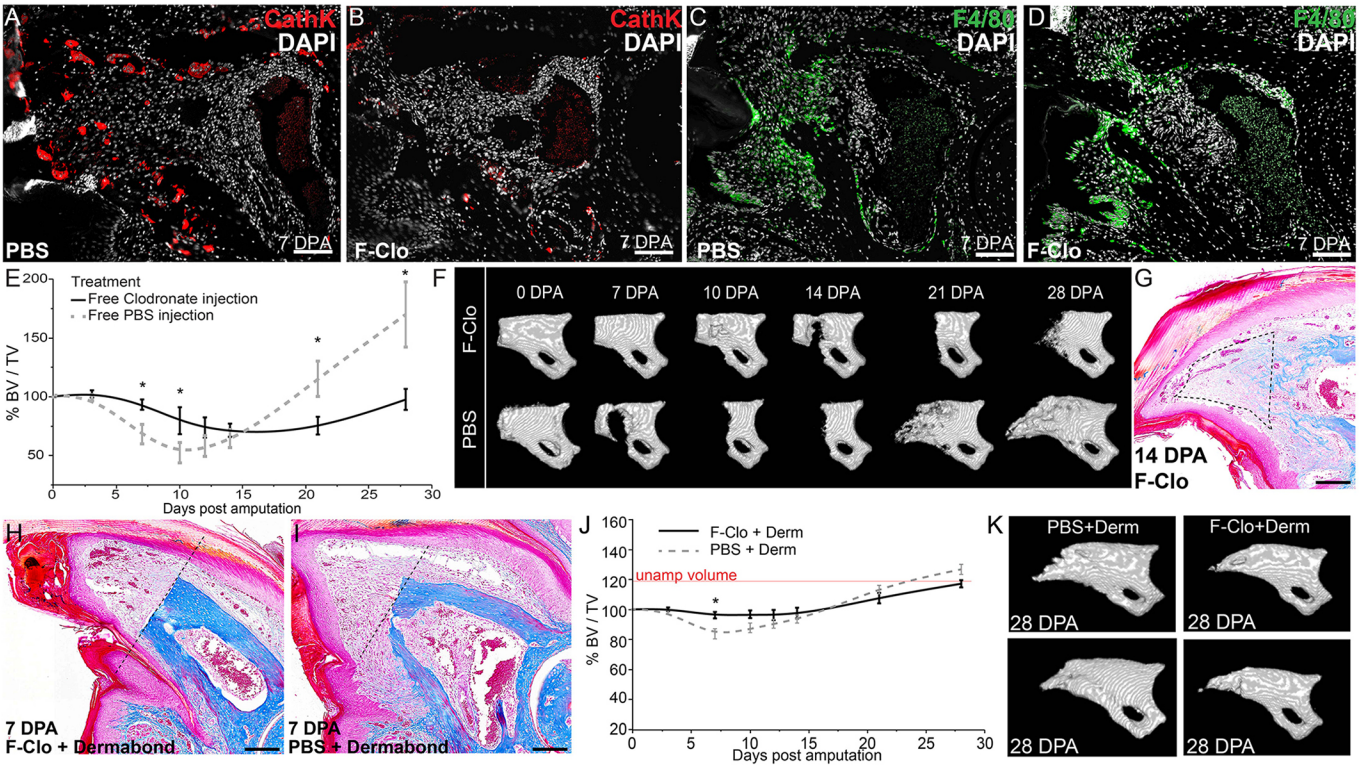

Fig. 5. Osteoclast-specific depletion delays but does not inhibit regeneration. (A,B) A single injection of free clodronate (F-Clo) immediately following amputation depletes the P3 digit of cathepsin K^{+} (CathK, red) cells. Representative image of a PBS-injected control digit (A) and a F-Clo injected digit (B) at 7 DPA. (C,D) F4/80^{+} staining (green) in PBS-injected digit (C) and F-Clo-injected digit (D) at 7 DPA showing macrophage localization to cells surrounding the bone stump. Gray, DAPI nuclear stain. (E) µCT analysis of bone volume changes with time after amputation in PBS-treated digits and F-Clo-treated digits. Changes are measured in percent bone volume/total volume at time of amputation (%BV/TV). *n*=4 mice, 16 digits for both groups, Bonferroni post-hoc test, **P*<0.05 main effect treatment at the time points indicated. Error bars indicate s.e.m. (F) 3D renderings of µCT images for PBS-treated and F-Clo-treated digits over time. (G) Trichrome staining of F-Clo-treated digit at 14 DPA showing complete re-epithelialization and accumulation of cells in the distal mesenchyme (outlined). (H,I) Digits were treated with either F-Clo and Dermabond (H) or PBS and Dermabond (I). Trichrome staining reveals a loss of bone degradation from the original plane of amputation (dashed line) in F-Clo+Dermabond-treated digits and only minor degradation in PBS+Dermabond-treated digits. (J) µCT to track bone volume changes measured in percent bone volume/total volume at time of amputation (%BV/TV). Digits were treated with combined F-Clo and Dermabond or with combined PBS and Dermabond. In both treatment groups, bone regenerates to pre-amputation levels (red line). *n*=4 mice, 16 digits for both groups. Bonferroni post-hoc test, **P*<0.05 main effect treatment. (K) Representative µCT images of P3 bone in either combined PBS and Dermabond treatment or combined F-Clo and Dermabond treatment groups at 28 DPA, showing patterned bone growth in both groups. For all images: distal, left; dorsal, top. Scale bars: 100 µm.

by 7 DPA, and in both cases a blastema formed distal to the stump bone (Fig. 5H,I) that resulted in a regenerated digit (Fig. 5J,K). µCT imaging of F-Clo/Dermabond-treated and PBS/Dermabond-treated digits showed that the amount of bone degradation was reduced in PBS-treated digits and completely inhibited in F-Clo-treated digits (Fig. 5J). Nevertheless, both PBS control and F-Clo-treated digits regenerated the amputated digit tip, suggesting that the absence of osteoclasts is not inhibitory for regeneration if re-epithelialization is allowed to occur.

Stimulating epidermal closure does not rescue Clo-Lipo inhibition of regeneration

Because rescue of re-epithelialization promotes a regenerative response in osteoclast-depleted digits, we next tested whether re-epithelialization could rescue regeneration in a macrophage-depleted (Clo-Lipo-injected) digit. We first established that Dermabond rescues the wound closure deficit that results from macrophage depletion and that re-epithelialization is complete by 7 DPA (Fig. 6A,B). Clo-Lipo/Dermabond-treated digits do not show evidence of bone degradation but develop a distal accumulation of cells (Fig. 6B). This aggregate of cells is not observed at a later time point (DPA 28, Fig. 6D). We used µCT imaging to track anatomical and bone volume changes of the digits during the regenerative response. In control studies combining Dermabond wound dressing with PBS-Lipo treatment we observed a regenerative response similar to that which occurs following only Dermabond treatment, whereas digits treated with Dermabond and Clo-Lipo displayed no change in stump bone volume or anatomy (Fig. 6C,D) indicating the absence of a regeneration response.

These studies show that rescuing wound closure is not sufficient to rescue the regeneration response caused by combined osteoclast/macrophage depletion. The data show that the wound epidermis is able to recruit cells to form a blastema-like accumulation of cells; however, this population of cells fails to progress to differentiated bone, indicating that the final stages of blastema differentiation are macrophage dependent. Overall, these studies indicate that osteoclasts and macrophages play a role in the early regeneration stages (i.e. re-epithelialization and bone degradation), but that macrophages specifically are required for final stages of digit regeneration (i.e. maintenance and differentiation of the blastema).

DISCUSSION

In adult mammals, the resolution of traumatic injury throughout the body is tissue specific: some tissues undergo impaired healing with

Development (2017) 144, 3907-3916 doi:10.1242/dev.150086

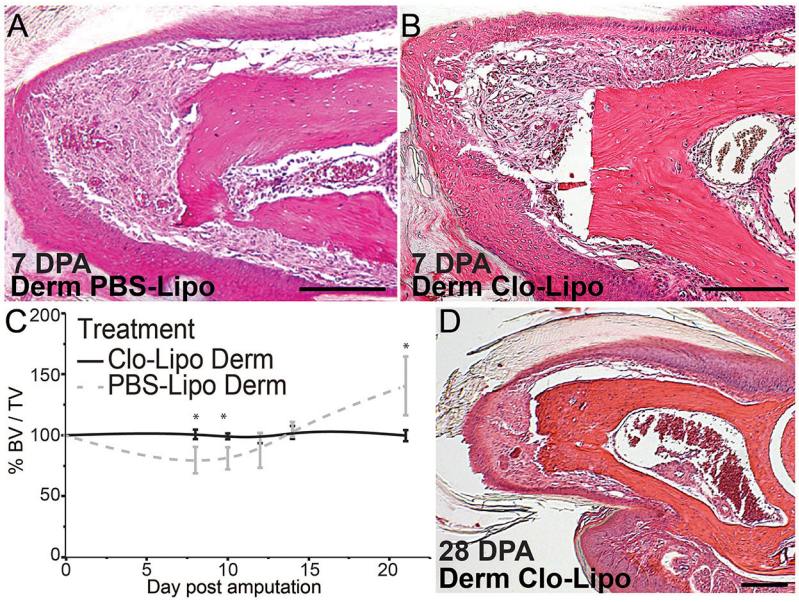

Fig. 6. Rescuing epidermal closure does not rescue regeneration in Clo-Lipo-treated digits. (A,B) H&E staining for histology shows that application of Dermabond promotes epidermal closure and accumulation of mesenchymal cells under the epidermis by 7 DPA in PBS-Lipo-treated digits (A) and Clo-Lipo-treated digits (B). (C) µCT analysis of bone volume change over time reveals a loss of regeneration response in Clo-Lipo-treated digits despite the rescue of epidermal closure. *y*-axis, percent bone volume over total volume at time of amputation (%BV/TV). *n*=8 digits for Clo-Lipo +Dermabond, *n*=4 digits for PBS-Lipo+Dermabond. Bonferroni post-hoc test, **P*<0.05 for main effect treatment at the time points indicated. Error bars indicate s.e.m. (D) H&E staining of Dermabond-treated, Clo-Lipo-injected digits at 28 DPA shows no evidence of bone degradation or regrowth. For all images: distal, left; dorsal, top. Scale bars: 100 µm.

little sign of regeneration (e.g. skin, heart), whereas other tissues are able to regenerate a functional replacement (e.g. bone, skeletal muscle, liver) (Stocum, 2012). In all of these tissues the injury response involves inflammation that includes the mobilization and invasion of macrophages. A key goal in regeneration biology is preventing pathological outcomes from uncontrolled infection or fibrosis and enhancing restoration of tissue function. Macrophages are essential in protecting the host from infection and have recently been shown to be essential in promoting regenerative responses (Godwin et al., 2013; Petrie et al., 2014). Our current study expands upon these experiments in salamanders and fish, providing evidence that macrophages are essential for epimorphic regeneration in mammals as well. Thus, these cells, as protectors from infection and promoters of repair, provide interesting targets for the field of regenerative medicine.

To use these cells as therapeutic interventions for regenerative medicine, the prominent question is one of timing; at what stage are macrophages necessary for an epimorphic regeneration response? In the current study, we used the regenerating digit tip of the mouse to show that macrophage invasion is essential for every stage of regeneration. Macrophage depletion causes an inhibition of osteoclastogenesis and bone degradation, re-epithelialization, blastema formation, and redifferentiation of the blastema to reform the digit tip. Rescue of these individual stages narrows down specific roles for macrophages during regeneration. We find macrophages are required for osteoclastogenesis and bone degradation, but our data suggest this process itself is not required for a successful regenerative response. On the other hand, we find that macrophages are essential for re-epithelialization of the wound, and the wound epidermis is required for blastema formation. Finally, macrophages are required for blastema cell differentiation in a manner independent of both degradation and re-epithelialization. Overall, the evidence suggests that epimorphic regeneration in a mammalian model is macrophage dependent and that macrophages regulate multiple key components of the regeneration response.

Osteoclasts and bone degradation are not required for regeneration

Osteoclasts are generally viewed as a bone-specific resident macrophage population, having the same progenitor cell as tissue macrophages (Sinder et al., 2015). Similar to previous studies of macrophage depletion in fracture healing (Alexander et al., 2011; Winkler et al., 2010), we find that Clo-Lipo injections effectively deplete both tissue macrophages and local osteoclasts, subsequently inhibiting both bone degradation and regeneration. Although it is clear that osteoclasts play a histolytic role in the regeneration response, it has not been clear whether the degradation of bone is required for a regenerative response. There is evidence implicating the bone degradation response in regulating blastema size and the extent of the regenerative response (Sammarco et al., 2015). Studies in other models of epimorphic regeneration show that histolytic activity is upregulated early in regeneration and that matrix metalloproteinase activity plays a role in regenerate patterning (Bai et al., 2005; Grillo et al., 1968; Vinarsky et al., 2005; Yang and Bryant, 1994; Yang et al., 1999). In mouse digit regeneration we provide evidence that wound closure signals the termination of the bone degradation phase and transitions the regeneration response to blastema formation (Simkin et al., 2015). Here we show that the use of clodronate to selectively deplete osteoclasts and delay degradation combined with enhancing wound closure to precociously terminate degradation completely eliminates bone degradation without depleting the macrophage population. The results show clearly that blastema formation and regeneration still occur under conditions in which there is no anatomical evidence of bone degradation. Thus it is clear that histolysis of the bone stump, although a prominent feature of the regeneration response, is not required for an epimorphic regenerative response in mice. In parallel, fracture healing studies show that osteoclast-specific inhibition in a tissue-specific model of bone regeneration does not inhibit the osteogenic response (Alexander et al., 2011).

The wound epidermis is required for blastema accumulation

Local depletion of macrophages during digit tip regeneration leads to a complete inhibition of re-epithelialization. Similar results from tissue-specific wound healing studies have been reported (Leibovich and Ross, 1975; Lucas et al., 2010; Mirza et al., 2009) indicating that macrophages are required for re-epithelialization in mammalian full-thickness wounds. In digit amputation, we have previously shown that re-epithelialization can be enhanced simply by treating the amputation wound with a cyanoacrylic wound

Development (2017) 144, 3907-3916 doi:10.1242/dev.150086

dressing, Dermabond (Simkin et al., 2015), and we show in the current study that Dermabond rescues re-epithelialization inhibited by macrophage and osteoclast depletion. Such rescue is consistent with the conclusion that macrophages play a role in creating a wound environment permissive for re-epithelialization rather than having a direct effect on epidermal cells. The lack of an apparent effect on epidermal expansion and nail elongation in macrophage-depleted digits also supports this conclusion.

Because macrophage depletion inhibits the formation of the wound epidermis, blastema formation and blastema differentiation we are able to explore the relationship between these events. Dermabond stimulates the formation of a wound epidermis and rescues regeneration in osteoclast-depleted digits but does not rescue regeneration in macrophage-depleted digits. In macrophage-depleted digits, the wound epidermis does stimulate the accumulation of a population of cells that appear blastema-like distal to the amputation stump. Although the regenerative potential of this structure will require further examination, these data suggest the wound epidermis plays a major role in recruiting cells distal to the amputation injury. We find that without macrophages these cells do not differentiate into new tissues of the digit. The necessity of the wound epidermal and mesenchymal cell interactions for epimorphic regeneration is established in other models such as salamander limb regeneration and zebrafish fin regeneration (Carlson, 1969; Chablais and Jazwinska, 2010; Goss, 1956; Mescher, 1976; Whitehead et al., 2005) and, in the mouse digit, WNT signaling derived from epidermal cells has been shown to be necessary for regeneration (Lehoczky and Tabin, 2015; Takeo et al., 2013). However, our studies suggest that macrophages are a necessary intermediate in these epidermal-mesenchymal interactions for complete digit regeneration.

Macrophages play multiple roles in epimorphic regeneration

During traumatic injury the inflammatory response must navigate a fine balance between the initial protection against infection versus the eventual promotion of a functional repair response (Godwin et al., 2016). In classical epimorphic regeneration models, such as the salamander limb or the zebrafish fin, recent macrophage depletion studies provide clear evidence that this balance is tipped toward the promotion of a functional regeneration response (Godwin et al., 2013; Petrie et al., 2014), and our study adds the mouse digit tip to this list of macrophage-dependent regenerative responses.

Epimorphic regeneration in adult mammals is relatively rare, whereas the regeneration of specific tissues such as muscle and bone can be robust. Other tissues, such as the skin, display regenerative responses only during specific developmental stages (fetal) or in selective regions of the body (e.g. oral skin), whereas adult skin typically undergoes a non-regenerative healing response that culminates in the deposition of scar tissue (Mak et al., 2009; Martin and Leibovich, 2005). It is interesting that the inflammation response is known to promote the regeneration of bone and muscle tissue, while inhibiting regenerative healing full-thickness skin wounds (Martin et al., 2003; Mori et al., 2008; Novak et al., 2014; Raggatt et al., 2014). These observations point to the evolution of an inflammatory balance between the initial protection against infection that drives the response in skin wounds versus the promotion of regenerative responses of internal tissues, such as muscle and bone, that is necessary for body function and survival. It is interesting that some of the macrophage activities identified in epimorphic regeneration parallel established tissue-specific responses of skin (e.g. promotion of re-epithelialization) and bone (e.g. promotion of osteogenesis). Thus, the data support the idea that what makes epimorphic regeneration unique is the way in which multiple tissue-specific responses are coordinated both temporally and spatially, and that macrophages play a key role in this process. This conclusion also helps to bridge the interface between epimorphic and tissue-specific regenerative responses, and provides an avenue for the development of strategies to enhance regeneration in mammals.

MATERIALS AND METHODS

Digit amputations and animal care

Adult 8-week-old female CD1 mice were obtained from Charles River Laboratories. Mice were anesthetized with 1-5% isoflurane gas with continuous inhalation. The second and fourth digits of both hind limbs were amputated at the P3 distal level as described previously (Simkin et al., 2013). Digits were collected at specified time points for histological analysis. All experiments were performed in accordance with the standard operating procedures approved by the Institutional Animal Care and Use Committees at Tulane University Health Sciences Center and the College of Veterinary Medicine at Texas A&M University.

Histology and immunohistochemistry

Tissue was harvested at specified time points and fixed in zinc-buffered formalin (Anatech) overnight. Bone was decalcified for 8 h in formic acid-based decalcifier (Decal I, Surgipath). Samples were processed for paraffin embedding using a Leica TP 1020 Processor. Serial sections (4 µm) were obtained using a Leica RM2255 microtome. Sections were deparaffinized in xylenes and rehydrated through a graded ethanol series. Mayer's Hematoxylin and Eosin Y (Sigma-Aldrich) (H&E) staining was carried out according to the manufacturer's protocol. Mallory's Trichrome staining was carried out according to the manufacturer's instructions (American Mastertech). Coverslips were mounted with Permount mounting medium (Fisher Scientific). For immunohistochemistry, serial sections were deparaffinized in xylene and rehydrated through graded ethanol. Antigen retrieval was carried out in either a pH 6 citrate buffer for 20 min at 90°C or with proteinase K at 10 mg/ml for 10 min at 37°C according to in-house optimized protocols for each antibody. Endogenous hydrogen peroxide was blocked using a solution of 3% H_2O_2 in methanol, and endogenous avidin and biotin were blocked with a Dako blocking kit. Non-specific antibody binding sites were blocked using a serum-free blocking buffer (Dako). Slides were incubated at 4°C overnight with the following primary antibodies: F4/80 (5 µg/ml, rat anti-mouse, 14-4801, eBioscience), Ly6B.2 (0.1 µg/ml, rat anti-mouse, MCA771A, AbD Serotec/Bio-Rad), cathepsin K (2 µg/ml, rabbit anti-mouse, 19027, Abcam) and CD45 (5 µg/ml, rat anti-mouse, 103101, BioLegend). Primary antibody detection was carried out using either secondary antibodies conjugated to Alexa Fluor 488 and 568 (Invitrogen) or secondary antibodies conjugated to biotin and resolved with a tyramide amplification kit according to the manufacturer's instructions (TSA kit T20912, Invitrogen/Thermo Fisher Scientific).

Image analysis

Brightfield images of histological sections were obtained using a 10×, 20× or 40× objective on an Olympus BX60 upright microscope equipped with an Olympus DP72 camera. Fluorescent micrographs were acquired on an Olympus BX61 fluorescence deconvolution microscope. Quantification of fluorescent signal was performed using masking subsampling of positive fluorescent area in Slidebook Imaging Software (Intelligent Imagine Innovations). Total area of 488 or 568 nm fluorescent signal was calculated and normalized to total DAPI area to calculate percentage positive area/total cellular area. Signal quantification was restricted to the connective tissue area, excluding nail, epidermis, scab, bone and bone marrow. The entire P3 area of a representative section of each sample was imaged for quantification at 10× magnification. Autofluorescent red blood cells were subtracted from images using a Slidebook subtraction algorithm before quantification to reduce background signal.

MCP1 bead implants

Cibacron Blue Affi-Gel agarose beads (400 µm, Bio-Rad) were soaked in 0.5 mg/ml MCP1 (Prospec, CHM-313) with 0.1% BSA in PBS. Vehicle control beads were soaked in 0.1% BSA in PBS. Bead implants were carried

Development (2017) 144, 3907-3916 doi:10.1242/dev.150086

out as previously described (Simkin et al., 2013). Briefly, after soaking in protein solution overnight, beads were allowed to air dry and were implanted using tungsten needles into the dermis surrounding the P3 bone at 0 or 3 DPA. For each treated mouse, digits on one paw received PBS-soaked beads and on the other paw MCP1-soaked beads. Left/right paw treatment was randomized for each mouse. Macrophage recruitment was calculated with immunofluorescent analysis as described above.

Osteoclast or macrophage depletion and rescue of re-epithelialization

For macrophage or osteoclast depletion, 10 µl 50 mg/ml clodronate liposomes (Clo-Lipo) or PBS liposomes (PBS-Lipo) (www.ClodronateLiposomes.com) was injected into the P2 region of each amputated digit using an insulin syringe. Each digit received an injection at 0, 2 and 5 DPA. For depletion of osteoclasts, clodronate (1.85 µg/g body weight) was injected in 10 µl PBS into the P2 region just prior to digit amputation. For control digits, 10 µl PBS was injected alone. Depletion efficacy was quantified by immunofluorescence for cathepsin K^+ and F4/80$^+$ cells. In rescue of wound closure experiments, 10 µl Dermabond (Ethicon) was applied to each digit immediately following amputation. Digits were allowed to dry for 1 min following Dermabond application and then injected with Clo-Lipo, PBS-Lipo, F-Clo or PBS.

Micro-CT (µCT) analysis

µCT images were acquired using a VivaCT 40 (Scanco Medical) at 1000 projections per 180° with a voxel resolution of 10 μm^3, and energy and intensity settings of 55 V and 145 µA, respectively. Integration time for capturing the projections was set to 380 ms using continuous rotation. Images were segmented using the BoneJ (Doube et al., 2010) (version 1.2.1) Optimize Threshold plugin for ImageJ (NIH, version 1.48c). Changes in bone volume were quantified using the BoneJ Volume Fraction plugin for ImageJ. Percent bone volume divided by total bone volume (% BV/TV) was calculated by normalizing the measurement of each digit to its original volume immediately following amputation. Final images were compiled using Adobe Photoshop CS4 and CS6.

Statistical analysis

Bone volume graphs were compiled and were analyzed using two-way ANOVA with main effects treatment and time using JMP (version 10.0.0, SAS Institute). Bonferroni multiple comparison tests were conducted for simple effect treatment at specific time points when appropriate and reported on the graphs. Graphs of immunopositive area for cell counting studies were compiled and analyzed using Prism (version 6, GraphPad). Two-way ANOVA with main effects time and treatment or unpaired Student's *t*-test for simple effect treatment were calculated as indicated in figure legends. All figures were compiled using Adobe Photoshop and Adobe Illustrator CS6.

Acknowledgements

We thank members of the K.M. lab, Larry Suva and Dana Gaddy for discussions.

Competing interests

The authors declare no competing or financial interests.

Author contributions

Conceptualization: K.M., J.S., M.C.S., L.M.; Methodology: J.S., M.C.S., L.M., M.Y.; Validation: M.Y.; Formal analysis: K.M., J.S., M.C.S., L.M., C.T., A.C.; Investigation: J.S., M.C.S., L.M., L.A.D., M.Y., C.T., A.C.; Writing - original draft: K.M., J.S., M.C.S.; Writing - review & editing: K.M., J.S., M.C.S., L.A.D., M.Y.; Visualization: J.S., M.C.S., L.M., M.Y.; Supervision: K.M.; Project administration: K.M.; Funding acquisition: K.M.

Funding

Funding for this project was provided by W911NF-06-1-0161 from Defense Advanced Research Projects Agency (DARPA), W911NF-09-1-0305 from the US Army Research Laboratory, the John L. and Mary Wright Ebaugh endowment fund at Tulane University, and Texas A&M University to K.M., and the Eunice Kennedy Shriver National Institute of Child Health and Human Development NIH-F32HD071763 to M.C.S. Deposited in PMC for release after 12 months.

Supplementary information

Supplementary information available online at
http://dev.biologists.org/lookup/doi/10.1242/dev.150086.supplemental

References

Alexander, K. A., Chang, M. K., Maylin, E. R., Kohler, T., Müller, R., Wu, A. C., Van Rooijen, N., Sweet, M. J., Hume, D. A., Raggatt, L. J. et al. (2011). Osteal macrophages promote in vivo intramembranous bone healing in a mouse tibial injury model. *J. Bone Miner. Res.* **26**, 1517-1532.

Ashcroft, G. S., Yang, X., Glick, A. B., Weinstein, M., Letterio, J. J., Mizel, D. E., Anzano, M., Greenwell-Wild, T., Wahl, S. M. and Deng, C. (1999). Mice lacking Smad3 show accelerated wound healing and an impaired local inflammatory response. *Nat. Cell Biol.* **1**, 260-266.

Austyn, J. M. and Gordon, S. (1981). F4/80, a monoclonal antibody directed specifically against the mouse macrophage. *Eur. J. Immunol.* **11**, 805-815.

Bai, S., Thummel, R., Godwin, A. R., Nagase, H., Itoh, Y., Li, L., Evans, R., McDermott, J., Seiki, M. and Sarras, M. P., Jr (2005). Matrix metalloproteinase expression and function during fin regeneration in zebrafish: analysis of MT1-MMP, MMP2 and TIMP2. *Matrix Biol.* **24**, 247-260.

Barrera, P., Blom, A., Van Lent, P. L. E. M., Van Bloois, L., Beijnen, J. H., Van Rooijen, N., De Waal Malefijt, M. C., Van de Putte, L. B. A., Storm, G. and Van den Berg, W. B. (2000). Synovial macrophage depletion with clodronate-containing liposomes in rheumatoid arthritis. *Arthritis. Rheum.* **43**, 1951-1959.

Borgens, R. B. (1982). Mice regrow the tips of their foretoes. *Science* **217**, 747-750.

Brockes, J. P. (1997). Amphibian limb regeneration: rebuilding a complex structure. *Science* **276**, 81-87.

Brockes, J. P. and Kumar, A. (2002). Plasticity and reprogramming of differentiated cells in amphibian regeneration. *Nat. Rev. Mol. Cell Biol.* **3**, 566-574.

Bryant, S. V., Endo, T. and Gardiner, D. M. (2002). Vertebrate limb regeneration and the origin of limb stem cells. *Int. J. Dev. Biol.* **46**, 887-896.

Carlson, B. M. (1969). Inhibition of limb regeneration in the axolotl after treatment of the skin with actinomycin D. *Anat. Rec.* **163**, 389-401.

Carlson, B. M. (2005). Some principles of regeneration in mammalian systems. *Anat. Rec. B New Anat.* **287B**, 4-13.

Chablais, F. and Jazwinska, A. (2010). IGF signaling between blastema and wound epidermis is required for fin regeneration. *Development* **137**, 871-879.

DiPietro, L. A., Burdick, M., Low, Q. E., Kunkel, S. L. and Strieter, R. M. (1998). MIP-1alpha as a critical macrophage chemoattractant in murine wound repair. *J. Clin. Investig.* **101**, 1693.

Dipietro, L. A., Reintjes, M. G., Low, Q. E. H., Levi, B. and Gamelli, R. L. (2001). Modulation of macrophage recruitment into wounds by monocyte chemoattractant protein-1. *Wound Repair Regen.* **9**, 28-33.

Doube, M., Kłosowski, M. M., Arganda-Carreras, I., Cordelières, F. P., Dougherty, R. P., Jackson, J. S., Schmid, B., Hutchinson, J. R. and Shefelbine, S. J. (2010). BoneJ: free and extensible bone image analysis in ImageJ. *Bone* **47**, 1076-1079.

Eming, S. A., Martin, P. and Tomic-Canic, M. (2014). Wound repair and regeneration: mechanisms, signaling, and translation. *Sci. Transl. Med.* **6**, 265sr6.

Fernando, W. A., Leininger, E., Simkin, J., Li, N., Malcom, C. A., Sathyamoorthi, S., Han, M. and Muneoka, K. (2011). Wound healing and blastema formation in regenerating digit tips of adult mice. *Dev. Biol.* **350**, 301-310.

Frith, J. C., Mönkkönen, J., Blackburn, G. M., Russell, R. G. G. and Rogers, M. J. (1997). Clodronate and liposome-encapsulated clodronate are metabolized to a toxic ATP analog, adenosine 5′-(β,γ-dichloromethylene) triphosphate, by mammalian cells in vitro. *J. Bone Miner. Res.* **12**, 1358-1367.

Gemberling, M., Bailey, T. J., Hyde, D. R. and Poss, K. D. (2013). The zebrafish as a model for complex tissue regeneration. *Trends Genet.* **29**, 611-620.

Godwin, J. W., Pinto, A. R. and Rosenthal, N. A. (2013). Macrophages are required for adult salamander limb regeneration. *Proc. Natl. Acad. Sci. USA* **110**, 9415-9420.

Godwin, J. W., Pinto, A. R. and Rosenthal, N. A. (2016). Chasing the recipe for a pro-regenerative immune system. *Semin. Cell Dev. Biol.* 61, 71-79.

Goren, I., Allmann, N., Yogev, N., Schürmann, C., Linke, A., Holdener, M., Waisman, A., Pfeilschifter, J. and Frank, S. (2009). A transgenic mouse model of inducible macrophage depletion: effects of diphtheria toxin-driven lysozyme M-specific cell lineage ablation on wound inflammatory, angiogenic, and contractive processes. *Am. J. Pathol.* **175**, 132-147.

Goss, R. J. (1956). Regenerative inhibition following limb amputation and immediate insertion into the body cavity. *Anat. Rec.* **126**, 15-27.

Grillo, H. C., Lapière, C. M., Dresden, M. H. and Gross, J. (1968). Collagenolytic activity in regenerating forelimbs of the adult newt (Triturus viridescens). *Dev. Biol.* **17**, 571-583.

Han, M., Yang, X., Lee, J., Allan, C. H. and Muneoka, K. (2008). Development and regeneration of the neonatal digit tip in mice. *Dev. Biol.* **315**, 125-135.

Hirsch, S. and Gordon, S. (1983). Polymorphic expression of a neutrophil differentiation antigen revealed by monoclonal antibody 7/4. *Immunogenetics* **18**, 229-239.

Illingworth, C. M. (1974). Trapped fingers and amputated finger tips in children. *J. Pediatr. Surg.* **9**, 853-858.

Khan, U. A., Hashimi, S. M., Bakr, M. M., Forwood, M. R. and Morrison, N. A. (2016). CCL2 and CCR2 are essential for the formation of osteoclasts and foreign body giant cells. *J. Cell. Biochem.* **117**, 382-389.

Kyriakides, T. R., Foster, M. J., Keeney, G. E., Tsai, A., Giachelli, C. M., Clark-Lewis, I., Rollins, B. J. and Bornstein, P. (2004). The CC chemokine ligand,

CCL2/MCP1, participates in macrophage fusion and foreign body giant cell formation. *Am. J. Pathol.* **165**, 2157-2166.
Lehoczky, J. A. and Tabin, C. J. (2015). Lgr6 marks nail stem cells and is required for digit tip regeneration. *Proc. Natl. Acad. Sci. USA* **112**, 13249-13254.
Leibovich, S. J. and Ross, R. (1975). The role of the macrophage in wound repair. A study with hydrocortisone and antimacrophage serum. *Am. J. Pathol.* **78**, 71-100.
Li, S., Li, B., Jiang, H., Wang, Y., Qu, M., Duan, H., Zhou, Q. and Shi, W. (2013). Macrophage depletion impairs corneal wound healing after autologous transplantation in mice. *PLoS ONE* **8**, e61799.
Lucas, T., Waisman, A., Ranjan, R., Roes, J., Krieg, T., Muller, W., Roers, A. and Eming, S. A. (2010). Differential roles of macrophages in diverse phases of skin repair. *J. Immunol.* **184**, 3964-3977.
Mak, K., Manji, A., Gallant-Behm, C., Wiebe, C., Hart, D. A., Larjava, H. and Häkkinen, L. (2009). Scarless healing of oral mucosa is characterized by faster resolution of inflammation and control of myofibroblast action compared to skin wounds in the red Duroc pig model. *J. Dermatol. Sci.* **56**, 168-180.
Martin, P. and Leibovich, S. J. (2005). Inflammatory cells during wound repair: the good, the bad and the ugly. *Trends Cell Biol.* **15**, 599-607.
Martin, P., D'Souza, D., Martin, J., Grose, R., Cooper, L., Maki, R. and McKercher, S. R. (2003). Wound healing in the PU.1 null mouse–tissue repair is not dependent on inflammatory cells. *Curr. Biol.* **13**, 1122-1128.
McKim, L. H. (1932). Regeneration of the distal phalanx. *Can. Med. Assoc. J.* **26**, 549-550.
Mescher, A. L. (1976). Effects on adult newt limb regeneration of partial and complete skin flaps over the amputation surface. *J. Exp. Zool.* **195**, 117-127.
Mirza, R., DiPietro, L. A. and Koh, T. J. (2009). Selective and specific macrophage ablation is detrimental to wound healing in mice. *Am. J. Pathol.* **175**, 2454-2462.
Mori, R., Kondo, T., Ohshima, T., Ishida, Y. and Mukaida, N. (2002). Accelerated wound healing in tumor necrosis factor receptor p55-deficient mice with reduced leukocyte infiltration. *FASEB J.* **16**, 963-974.
Mori, R., Shaw, T. J. and Martin, P. (2008). Molecular mechanisms linking wound inflammation and fibrosis: knockdown of osteopontin leads to rapid repair and reduced scarring. *J. Exp. Med.* **205**, 43-51.
Neufeld, D. A. and Zhao, W. (1993). Phalangeal regrowth in rodents: postamputational bone regrowth depends upon the level of amputation. *Prog. Clin. Biol. Res.* **383A**, 243-252.
Novak, M. L., Weinheimer-Haus, E. M. and Koh, T. J. (2014). Macrophage activation and skeletal muscle healing following traumatic injury. *J. Pathol.* **232**, 344-355.
Petrie, T. A., Strand, N. S., Tsung-Yang, C., Rabinowitz, J. S. and Moon, R. T. (2014). Macrophages modulate adult zebrafish tail fin regeneration. *Development* **141**, 2581-2591.
Pfefferli, C. and Jaźwińska, A. (2015). The art of fin regeneration in zebrafish. *Regeneration* **2**, 72-83.
Raggatt, L. J., Wullschleger, M. E., Alexander, K. A., Wu, A. C. K., Millard, S. M., Kaur, S., Maugham, M. L., Gregory, L. S., Steck, R. and Pettit, A. R. (2014). Fracture healing via periosteal callus formation requires macrophages for both initiation and progression of early endochondral ossification. *Am. J. Pathol.* **184**, 3192-3204.
Russell, R. G. G. and Rogers, M. J. (1999). Bisphosphonates: from the laboratory to the clinic and back again. *Bone* **25**, 97-106.
Sammarco, M. C., Simkin, J., Fassler, D., Cammack, A. J., Wilson, A., Van Meter, K. and Muneoka, K. (2014). Endogenous bone regeneration is dependent upon a dynamic oxygen event. *J. Bone Miner. Res.* **29**, 2336-2345.
Sammarco, M. C., Simkin, J., Cammack, A. J., Fassler, D., Gossmann, A., Marrero, L., Lacey, M., Van Meter, K. and Muneoka, K. (2015). Hyperbaric oxygen promotes proximal bone regeneration and organized collagen composition during digit regeneration. *PLoS ONE* **10**, e0140156.
Schindeler, A., McDonald, M. M., Bokko, P. and Little, D. G. (2008). Bone remodeling during fracture repair: the cellular picture. *Semin. Cell Dev. Biol.* **19**, 459-466.
Simkin, J., Han, M., Yu, L., Yan, M. and Muneoka, K. (2013). The mouse digit tip: from wound healing to regeneration. *Methods Mol. Biol.* **1037**, 419-435.
Simkin, J., Sammarco, M. C., Dawson, L. A., Tucker, C., Taylor, L. J., Van Meter, K. and Muneoka, K. (2015). Epidermal closure regulates histolysis during mammalian (Mus) digit regeneration. *Regeneration* **2**, 106-119.
Sinder, B. P., Pettit, A. R. and McCauley, L. K. (2015). Macrophages: their emerging roles in bone. *J. Bone Miner. Res.* **30**, 2140-2149.
Sprangers, S., de Vries, T. J. and Everts, V. (2016). Monocyte heterogeneity: consequences for monocyte-derived immune cells. *J. Immunol. Res.* **2016**, 1475435.
Stocum, D. L. (2012). *Regenerative Biology and Medicine*. Amsterdam: Academic Press.
Stocum, D. L. and Cameron, J. A. (2011). Looking proximally and distally: 100 years of limb regeneration and beyond. *Dev. Dyn.* **240**, 943-968.
Takeo, M., Chou, W. C., Sun, Q., Lee, W., Rabbani, P., Loomis, C., Taketo, M. M. and Ito, M. (2013). Wnt activation in nail epithelium couples nail growth to digit regeneration. *Nature* **499**, 228-232.
Tanaka, E. M. (2003). Regeneration: if they can do it, why can't we? *Cell* **113**, 559-562.
van Rooijen, N. and Hendrikx, E. (2010). Liposomes for specific depletion of macrophages from organs and tissues. *Methods Mol. Biol.* **605**, 189-203.
Vinarsky, V., Atkinson, D. L., Stevenson, T. J., Keating, M. T. and Odelberg, S. J. (2005). Normal newt limb regeneration requires matrix metalloproteinase function. *Dev. Biol.* **279**, 86-98.
Whitehead, G. G., Makino, S., Lien, C.-L. and Keating, M. T. (2005). fgf20 is essential for initiating zebrafish fin regeneration. *Science* **310**, 1957-1960.
Winkler, I. G., Sims, N. A., Pettit, A. R., Barbier, V., Nowlan, B., Helwani, F., Poulton, I. J., van Rooijen, N., Alexander, K. A., Raggatt, L. J. et al. (2010). Bone marrow macrophages maintain hematopoietic stem cell (HSC) niches and their depletion mobilizes HSCs. *Blood* **116**, 4815-4828.
Xiang, S., Dong, H.-H., Liang, H.-F., He, S.-Q., Zhang, W., Li, C.-H., Zhang, B.-X., Zhang, B.-H., Jing, K., Tomlinson, S. et al. (2012). Oval cell response is attenuated by depletion of liver resident macrophages in the 2-AAF/partial hepatectomy rat. *PLoS ONE* **7**, e35180.
Xue, M. and Jackson, C. J. (2015). Extracellular matrix reorganization during wound healing and its impact on abnormal scarring. *Adv. Wound Care* **4**, 119-136.
Yang, E. V. and Bryant, S. V. (1994). Developmental regulation of a matrix metalloproteinase during regeneration of axolotl appendages. *Dev. Biol.* **166**, 696-703.
Yang, E. V., Gardiner, D. M., Carlson, M. R. J., Nugas, C. A. and Bryant, S. V. (1999). Expression of Mmp-9 and related matrix metalloproteinase genes during axolotl limb regeneration. *Dev. Dyn.* **216**, 2-9.
Zeisberger, S. M., Odermatt, B., Marty, C., Zehnder-Fjällman, A. H. M., Ballmer-Hofer, K. and Schwendener, R. A. (2006). Clodronate-liposome-mediated depletion of tumour-associated macrophages: a new and highly effective antiangiogenic therapy approach. *Br. J. Cancer* **95**, 272-281.